American Mineralogist, Volume 59, pages 261–273, 1974

Synthetic Sodium Phlogopite and Its Two Hydrates: Stabilities, Properties, and Mineralogic Implications

JOHN H. CARMAN

Department of Geology, University of Iowa, Iowa City, Iowa 52242

Abstract

Based on experimental studies of the $NaAlSiO_4$–Mg_2SiO_4–SiO_2–H_2O system, three previously undescribed synthetic sheet silicates are inferred to have the same oxide ratio, $Na_2O \cdot 6MgO \cdot Al_2O_3 \cdot 6SiO_2$, but different water contents. The lowest hydrate, represented by $NaMg_3AlSi_3O_{10}(OH)_2$, is monoclinic ($\beta = 97°\ 45'$, $a = 5.26$ Å, $b = 9.20$ Å, $c = 9.99$ Å, and $V = 479.8$ Å^3) and referred to as sodium phlogopite. Its maximum stability passes through 818°C at 250 bars and 874°C at 530 bars, beyond which it decomposes to forsterite, nepheline, albite, and vapor. Above a line through the point at 530 bars and another at 1100 bars and 960°C it decomposes to forsterite, nepheline, liquid, and vapor. Likewise, above a line connecting the point at 1100 bars and one at 5000 bars and 1010°C it decomposes to forsterite, liquid, and vapor.

At lower temperatures sodium phlogopite and water-rich vapor react to form sodium phlogopite hydrate I, represented by $NaMg_3AlSi_3O_{10}(OH)_2 \cdot 2H_2O$. It is monoclinic ($\beta = 98°\ 24'$, $a = 5.25$ Å, $b = 9.23$ Å, $c = 12.00$ Å, and $V = 575.8$ Å^3) and decomposes to sodium phlogopite and vapor above a line defined by $T = 17.4\ P + 328\ (\pm 2)$, where T is in °C and P is in kbar. Below this line, it is stable under water-saturated conditions, until below a line indicated by $T = 5.4\ P + 82\ (\pm 2)$ (T and P as above) where it combines with water to form $NaMg_3AlSi_3O_{10}(OH)_2 \cdot 5H_2O$. This material, here called sodium phlogopite hydrate II, is monoclinic ($\beta = 97°\ 28'$, $a = 5.33$Å, $b = 9.22$ Å, $c = 15.00$ Å, and $V = 730.0$ Å^3) and is the typical product of all water-saturated runs, because neither sodium phlogopite nor its hydrate I is quenchable under these conditions.

These results necessitate a reinterpretation of previous studies in this system in which synthetic montmorillonites of unusually high thermal stability were noted.

The structure and physical properties of sodium phlogopite resemble those of phlogopite and are qualitatively similar to those of vermiculite and montmorillonite without interlayer water. The two stages of interlayer hydration generally recognized for vermiculites and montmorillonites are similar to the two hydrates of sodium phlogopite both in structure and in pressure-temperature stability. Moreover, because chemically analyzed phlogopites, biotites, vermiculites, and montmorillonites contain potential amounts of sodium phlogopite and/or its hydrates, these latter may be useful as end-members in the interpretation of the physical, chemical, and genetic aspects of these natural sheet silicates. There are, however, no known occurrences of sodium phlogopite or its hydrates.

Introduction

The end-member concept has become invaluable to mineralogists who would hope to interrelate complex variations in physical properties of minerals to their complex compositions. When the physical properties and stabilities of enough end-members and the relations among them are known, geochemists and petrologists are often able to interpret geologic processes.

In this spirit, the physical properties and stabilities of three previously undescribed synthetic substances are presented and their implications relative to previous studies in the $NaAlSiO_4$-Mg_2SiO_4-SiO_2-H_2O system and mineralogy are interpreted. While the sheet silicates described do not occur naturally in pure form, it seems likely that they may serve as useful end-members for a better understanding of several groups of sheet silicates.

Previous Studies

Ames and Sand (1958) were apparently the first to encounter hydrated sodium-magnesium-aluminum-silicates at high P-T conditions in the Na_2O-MgO-

Al_2O_3-SiO_2-H_2O system. They referred to these water-expandable and ethylene glycol-expandable substances as montmorillonites in spite of the high temperatures involved (up to 750°C) and the high water contents implied by this term. Later studies by Koizumi and Roy (1959) and by Iiyama and Roy (1963a, 1963b) continued and refined this reference to montmorillonite ("montmorillonoid" and "saponite") for temperatures as high as 850°C at 1000 bars. They were able to demonstrate for these products reasonable indifference to time and some indifference to initial constitution (Iiyama and Roy, 1963a, pp. 18–19). While there is no doubt that their *products* were montmorillonite-like in chemical composition and physical properties, there is some question about the *amount of hydration* at the conditions of their experiments because their DTA results (Iiyama and Roy 1963a, Fig. 7) indicate all but (OH)-water is lost by 200°C at atmospheric pressure. In fact, Gillery (1959) was able to document that the basal spacings of material synthesized by Iiyama (see Iiyama and Roy, 1963a) had basal spacing between 10 and 11 Å at 350°C and atmospheric pressure, but at room temperature and atmospheric pressure they had basal spacings of either 12 Å, at low relative humidity, or 15 Å, at high relative humidity.

Sodic montmorillonite ($Na_{0.5}Mg_3Al_{0.5}Si_{3.5}O_{10}(OH)_2 \cdot nH_2O$), encountered by Ernst (1961) in his investigation of synthetic glaucophane, was inferred to be metastable at temperatures as high as 850°C at 2000 bars because glaucophane, $Na_2Mg_3Al_2Si_8O_{22}(OH)_2$, was shown to grow at its expense (Ernst, 1961, Fig. 1). This inference can be questioned because these two phases cannot be related by either a unary or a binary reaction as implied. Kushiro (1972, p. 316) accepted Ernst's argument by ignoring the phase relations of the "sodic montmorillonite" which he encountered in the $NaAlSiO_4$-Mg_2SiO_4-SiO_2-H_2O system at temperatures below 1000° C and high pressures. Needless to say the author might have chosen the same argument had he not been urged to do a systematic study of the $NaAlSiO_4$-Mg_2SiO_4-SiO_2-H_2O by O. F. Tuttle (Carman, 1969).

Methods

Externally-heated hydrothermal equipment (after Tuttle, 1949) and internally-heated gas equipment (after Yoder, 1950) were used for all quench-method experiments at elevated pressures. These systems were calibrated using Au and/or NaCl (Clark, 1959) so that temperatures are believed to be accurate to ± 10°C for controlled experiments. Pressures were referred to a Harwood manganin cell and are believed to be accurate to ± 70 bars. Starting materials included gels made using the techniques of Luth and Ingamells (1965), a gel mixture, and glasses made from gels or crystalline assemblages synthesized from gels (see Table 1 for compositions). Starting materials were encapsulated in gold or platinum with known amounts of distilled, deionized, and freshly boiled water. Individual quench runs were brought to temperature and lowered in temperature under pressure. The products were examined optically and by powder X-ray diffraction for gross textures and phase content.

Differential thermal analysis (DTA) under controlled pressure, after the technique of Yoder (1950), was used to study the stability of hydrated phases. Experimental material was encapsulated in pressure-transmitting gold containers (see, for method, Ernst, 1960, and Wones, 1967) with a reentrant well for a sheathed, ungrounded, chromel-alumel thermocouple. Lake Toxaway quartz, loaded into a similar container but open to the pressure system gas (Argon), served as a reference for the reactions studied. By using the experimental material as a reference, the *P-T* reaction determined by Yoder (1950) for α-quartz $\rightleftharpoons$ β-quartz served as a calibrant of the experimental system; experimental values attained were within ± 5°C or ± 275 bars of his determinations. Thermal effects, temperature and pressure were recorded on a millivolt recorder with the assistance of J. R. Weidner (University of Maryland). Heating and cooling rates between 1° and 10°/min were typical of the manual control used.

Controlled ignition was used to determine the water content of phases at various temperatures. An open platinum capsule in a sealable glass vial, an analytical balance (±0.01 mg), and standard laboratory equipment for heating and cooling were used.

A simple X-ray furnace was constructed to determine cell parameters of phases not stable at laboratory temperatures and relative humidities.

Experimental Results

Quench Data

Quench-method experiments in the SiO_2-poor part of the $NaAlSiO_4$-Mg_2SiO_4-SiO_2-H_2O system using

the compositions of Table 1 between 800°C to 1100°C and at pressures up to 5000 bars gave products identified as albite, nepheline, enstatite, forsterite, a minor amount of unknown silicate which may be amphibole, quench silicate-rich liquid, quench H_2O-rich vapor, and a highly hydrated sheet silicate, which constitutes one of the focal items of this report. The albite (Ab), nepheline (Ne), enstatite (En), and forsterite (Fo) could readily be identified by their characteristic habits, refractive indices and X-ray diffraction patterns as essentially pure compounds. When these were present in the final products of the experiments (Table 2), except for nepheline they were assumed to have formed during the experiment and to have persisted unchanged through the quench. By contrast, nepheline occurred in two distinct habits. The stubby hexagonal prisms, 5–30 microns in size, probably represent the primary unaltered form; the large spherulites (20–600 microns) which could be crushed into smaller irregular fragments with undulose extinction probably represent nepheline formed during the quench (qNe for run 1774, Table 2). The minor amount of questionable amphibole (recorded as Am? in runs 990 and 1251 of Table 2) resembled En but is thought to be an amphibole because of its higher birefringence, lower refractive indices (*ca* 1.60), and its small extinction angle. No significance can be placed on this phase because of its irregular occurrence. The colorless silicate glass could in most instances be interpreted to be quench silicate-rich liquid (L) which was stable at the conditions of the experiment. In other cases it was inferred to be a relict of the starting material which persisted during the experiment; such occurrences are referred to as metastable (see runs 1666 and 1915, Table 2). When glass was abundant, the whole charge was typically converted into a single glassy pellet which was extremely difficult to crush for microscopic examination. Surface features of this glassy pellet and its cohesiveness (or lack of it) have a bearing on other phases and products formed during the quench; quench H_2O-rich vapor is one of these. Water was usually present as liquid or droplets of liquid around glassy pellets in L-rich products. These pellets typically had at least one smoothly finished part to their surface which could be inferred to have been a meniscus contact between L and H_2O-rich vapor (V) during the experiment. Water is less obvious in crystal-rich products but can be observed as a transient dampness of the charge. In addition to

TABLE 1. Compositions of Gel Starting Materials

Comp. No.	$NaAlSiO_4$	Mg_2SiO_4	SiO_2	Comments
8	--	87.5	12.5	"Serpentine" *
60	45.0	30.0	25.0	
61	50.0	15.0	35.0	
63	61.0	8.0	31.0	
65	75.0	2.0	23.0	
67	75.0	15.0	10.0	
68	85.0	6.5	8.5	
69	100.0	---	---	Nepheline
71	75.0	25.0	---	
73	85.0	13.0	2.0	
74	67.5	5.0	27.5	
75	75.0	9.0	16.0	
76	60.0	5.0	35.0	
77	43.0	50.0	7.0	
78	34.5	51.5	14.0	
80-GG	37.1	55.1	7.8	Gel Mixture **
80	37.1	55.1	7.8	"Sodium Phlogopite" *
	(37.56)	(56.64)	(5.66)	Anal. of 80 ***
81†	39.0	59.0	2.0	
82	31.5	60.0	8.5	
87	18.0	78.0	4.0	

* Anhydrous mixture for hydrous phase
** 37.1 wt. % Gel #69 + 62.9 wt. % Gel #8
*** Also contains 0.13 wt. % Al_2O_3 (excess), 0.03 wt. % Fe_2O_3, 0.01 wt.% TiO_2, 0.11 wt. % CaO, 0.00 wt. % K_2O, < 0.01 wt. % Li_2O but no spectrographically detectible Sr, Br, Cr, Be, V, Ni, Ba, Mn or Zr, analyst C.O. Ingamells, No. 5-172, Mineral Constitution Laboratory, Pennsylvania State University.
† Run data on this composition indicate that it is more SiO_2-rich, about 10 wt.% SiO_2 while the Ne:Fo ratio was apparently the same.

water, minor amounts of low index spheres (1–3 microns) were observed, and sodium-rich or magnesium-rich phases may be observed where water was evaporated. Apparently the spheres are silicate-rich portions of the quenched vapor and evaporation of the water-rich part under atmospheric conditions yields the carbonated phases which occur *on* capsule walls and *on* glassy pellets. Magnesite rombs, nahcolite ($NaHCO_3$) as prisms and elbow-twins (Winchell and Winchell, 1964, p. 89), and flat spherulitic aggregates (5–50 microns in size) of Na_2CO_3-hydrates (?) have been noticed. Peters, Luth, and Tuttle (1966) observed similar sodium-rich products and spheres and posed a similar origin for them; thus, these phases are not listed among the results in Table 2.

The highly hydrated sheet silicate phase, mentioned above, was soon discovered to have three different structures, easily distinguished using X-ray diffraction, which were related to temperature and humidity at atmospheric pressure. At a relative humidity of about 30 percent, a 10 Å basal reflection resulted above 75 ± 5°C and persisted to at least 620°C. Between 75°C and 40 ± 3°C, a 12 Å basal reflection resulted. At lower temperatures, typical of lab conditions, the basal reflection was 15 Å. These same transition temperatures were noted on four different run products (2250 and 1251 of Table 2 and duplicates of these runs not recorded here); they were quickly and reversibly obtained with no indication of change in basal reflection between

transition temperatures or with time at constant temperature. This was interpreted to mean that the phase stable in high temperature runs could be the 10 Å phase regardless of the quenched product which was typically the 15 Å but sometimes the 12 Å phase. At the same time enough phase results were available on known compositions (Table 1) to suggest that this 10 Å mica had a high *P-T* stability and an oxide ratio of $Na_2O \cdot 6MgO \cdot Al_2O_3 \cdot 6SiO_2$. This stability and ratio suggested that it could be a sodium analog of phlogopite, $K_2O \cdot 6MgO \cdot Al_2O_3 \cdot 6SiO_2 \cdot 2H_2O$ or $KMg_3AlSi_3O_{10}(OH)_2$, so the provisional formula of $NaMg_3AlSi_3O_{10}(OH)_2$ was assumed and referred to as sodium phlogopite (SPh). Accordingly, its hydrates were referred to as sodium phlogopite hydrate I (SPh HI), the 12 Å phase, and sodium phlogopite hydrate II (SPh HII), the 15 Å phase, because of the evidence mentioned above that these phases differed only in regard to their water contents (SPh < SPh HI < SPh HII).

SPh and its hydrates were quite distinctive in quench products. All three are talc-like in softness

TABLE 2. Crucial Quench-Method Data Relevant to Stability of SPh

Run No.	Comp. No.	Start. Cond.*	Wt.% H_2O	Press. (bars)	Temp. (°C)	Time (hrs.)	Results†
REACTION 4	SPh=Fo+Ne+Ab+V						
1295	80	1251	5.9	276	800	67	SPh+V
1301	80	GG	6.0	276	825	257	SPh+(Fo)?+(Ne)?+V
1497	80	gel	23.9	296	830	597	Fo+Ne+Ab+V
1555	80	gel	23.9	276	840	254	Fo+Ne+Ab+V
2355	81	2250	33.2	276	845	112	Fo+Ne+(SPh)+V
2353	81	2190	28.8	276	355	167	Fo+Ne+(SPh)?+V
1505	81	2310	20.8	290	865	116	Fo+Ne+Ab+V
1707	80	gel	23.0	414	801	48	SPh+Ne+Fo+V
2311	81	2250	38.4	414	875	135	Fo+Ne+Ab+V
1549	80	gel	18.8	469	856	264	Fo+Ne+(SPh)?+(Ab)?+V
2350	81	2250	11.6	482	868	88	Fo+Ne+Ab+(SPh)+V
2351	81	2349	50.6	482	868	88	Fo+Ne+Ab+V
		Synthesis Runs for Reactions 4, 6 and 10					
2190	81	gel	0	1	1000	95	Fo+Ne+Ab
2349	81	2250	0	1	1000	50	Fo+Ne+Ab
2250	81	gel	20	1035	800	37	SPh+En+Ab?+V
2310	81	gel	20	1035	800	106	SPh+En+Fo+V
1251	80	GG	20	1035	700	336	SPh+Am?+V
1634	80	gel	20	1210	833	92	SPh+Fo+Ne+V
990	80	GG	20	2070	800	42	SPh+Am?+V
REACTION 5	Fo+Ne+Ab+V=L						
1718	65	828	23.8	414	897	40	Ne+Ab+Fo+V
1713	65	828	28.7	423	950	23	L+Ne+Fo+V
1667	76	gel	18.8	482	923	38	L+Ab+Fo+V
		Synthesis Runs for Reaction 5					
682	65	gel	5	551	840	40	Ne+Ab+SPh+(Fo)+V
828	65	682	0	1	1000	18	Ne+Ab+Fo

* Start. Cond. refers to starting condition, whether gel, gel mixture (GG) or previous run whose phases are indicated under synthesis runs.

† Results indicate phases in order of abundance with minor phases underlined (<5%), except V which placed as the last stable run phase. Quench phases preceeded by a "q" and inferred metastable phases enclosed in parenthesis. Question mark denotes uncertain identification of a phase, usually due to the amount present, or uncertain inference.. Abbreviations given in text along with descriptions of phases.

TABLE 2, continued

Run No.	Comp. No.	Start. Cond.*	Wt.% H_2O	Press. (bars)	Temp. (°C)	Time (hrs.)	Results†
REACTION 6	SPh=Fo+Ne+L+V						
2281	81	2250	15.5	551	890	90	Fo+Ne+L+V
1488	80	gel	23.8	690	880	589	Fo+Ne+SPh+V
2279	81	2250	12.4	759	910	48	Fo+Ne+L+V
1666	80	gel	29.9	759	887	62	Fo+Ne+SPh+(L)+V
2407	81	2349	3.26	759	905	76	Fo+Ne+L+(SPh)+V
2408	81	2310	3.42	759	905	76	Fo+Ne+L+(SPh)+V
1914	80	1634	24.4	1035	950	88	SPh+Fo+Ne+(L?)+V
1915	80	gel	19.7	1035	950	88	Fo+Ne+SPh+(L)+V
2140	80	gel	16.5	1035	975	75	Fo+L+Ne+V
2141	80	1634	19.6	1035	975	75	Fo+L+Ne+V
REACTION 7	SPh+Ab=Fo+L+V						
1486	60	994	33.4	690	880	589	Fo+L+Ab+V+qSPh
1739	63	832	22.6	741	888	48	L+Ab+Fo+V+qSPh
1891	78	gel	14.8	827	852	720	SPh+Fo+Ab+(L?)+V
1825	76	gel	25.8	827	874	59	L+Ab+SPh+V
1541	60	994	35.9	1035	825	168	SPh+Ab+V
1063	60	833	14.6	1035	837	102	SPh+Ab+V
1638	76	gel	30.4	1035	875	42	L+Ab+SPh+V
1640	78	gel	25.5	1035	875	42	SPh+Fo+Ab+(L?)+V
1839	61	gel	28.1	1035	876	83	Ab+(SPh)?+(Fo)?+(L)?+V
1102	60	gel	10.2	1035	900	60	L+Fo+V+qSPh
1103	62	gel	9.8	1035	900	60	L+Ab+Fo+V+qSPh
1104	63	gel	10.0	1035	900	60	L+SPh+Fo+V+qSPh
537	61	gel	20	1655	875	58	L+SPh+Fo+V+qSPh
538	60	gel	20	1655	875	58	SPh+L+Fo+V+qSPh
		Synthesis Runs for Reaction 7					
680	63	gel	5	552	840	40	Ab+Ne+SPh+(Fo)+V
677	60	gel	5	552	840	40	Ab+Ne+Fo+V
832	63	680	0	1	1000	19	Ab+Ne+Fo
833	60	677	0	1	1000	19	Ab+Ne+Fo
994	60	gel	20	690	800	48	Ab+SPh+V
REACTION 8	SPh+Ab+Ne=Fo+L, vapor-absent reaction, not studied.						
REACTION 9	SPh+Ab+Ne+V=L						
1818	65	828	31.1	690	858	720	L+Ne+SPh+(Ab?)+V
2037	74	gel	19.5	827	825	131	Ab+Ne+SPh+V
2030	74	gel	20.7	1035	801	179	Ab+Ne+SPh+V
1064	62	831	14.2	1035	837	102	L+Ab+SPh+V
1065	63	832	12.8	1035	837	102	Ab+SPh+L+V
1066	65	828	16.6	1035	837	102	L+Ne+SPh+V
2050	65	828	20.4	1380	797	593	Ne+L+SPh+V
2051	74	gel	22.2	1380	797	593	L+SPh+Ne?+V
		Synthesis Runs for Reaction 9					
828	65	682	0	1	1000	18	Ne+Ab+Fo
831	62	679	0	1	1000	19	Ab+Ne+Fo
832	63	680	0	1	1000	19	Ab+Ne+Fo
679	62	gel	5	552	840	40	Ab+Ne+Fo+L+V
680	63	gel	5	552	840	40	Ab+Ne+SPh+(Fo)+V
682	65	gel	5	552	840	40	Ne+Ab+(Fo)+SPh+V
REACTION 10	SPh=Fo+L+V						
1777	81	gel	34.8	2000	975	46	SPh+Fo+L+V
1853	77	gel	35.4	2205	975	71	SPh+Fo+L+V+qSPh
1854	78	gel	25.2	2205	975	71	Fo+L+V+qSPh
1856	80	gel	31.3	2205	975	71	SPh+Fo+L+V
1857	80	1634	25.2	2205	975	71	SPh+Fo+L+V
1858	81	gel	29.1	2205	975	71	SPh+Fo+L+V
1043	80	GG	4.4	2035	1000	24	Fo+L+V
1876	77	gel	32.4	2070	1000	16	Fo+L+V+qSPh
1877	78	gel	28.2	2070	1000	16	Fo+L+V
1879	80	gel	28.7	2070	1000	16	Fo+L+V+qSPh
1880	80	1634	29.8	2070	1000	16	Fo+L+V+qSPh
1881	81	gel	25.0	2070	1000	16	Fo+L+V+qSPh
1924	80	gel	25.4	2550	1000	66	Fo+L+V
1598	81	2349	24.2	3170	955	105	SPh+Fo+L+V
1599	81	2310	23.9	3170	955	105	SPh+Fo+L+V
1652	81	2310	23.3	3170	1025	24	Fo+L+V+qSPh
1653	81	2349	22.4	3170	1025	24	Fo+L+V+qSPh
1764	80	gel	31.4	4960	1000	40	SPh+Fo+L+V+qSPh
1765	80	1634	31.7	4960	1000	40	SPh+Fo+L+V+qSPh
1866	75	gel	21.1	4960	1000	79	L+SPh+V+qSPh
1867	77	gel	20.4	4960	1000	79	SPh+Fo+L+V+qSPh
1878	80	1634	19.1	4960	1000	79	SPh+Fo+L+V+qSPh
1869	80	gel	14.9	4960	1000	79	SPh+Fo+L+V+qSPh
1870	81	gel	19.0	4960	1000	79	SPh+Fo+L+V+qSPh
1871	82	gel	22.6	4960	1000	79	SPh+Fo+L+V+qSPh
1872-1	87	gel	18.9	4960	1000	79	Fo+SPh+V
1965	75	gel	18.6	5100	1015	81	L+Fo+V+qSPh
1966	77	gel	21.4	5100	1015	81	L+Fo+V+qSPh
1967	78	gel	21.7	5100	1015	81	L+Fo+V+qSPh
1968	80	1634	18.8	5100	1015	81	L+Fo+V+qSPh
1969	82	gel	20.2	5100	1015	81	L+Fo+V+qSPh
1077	80	990	20.3	5380	1110	6	L+Fo+V+qSPh
		See Reaction 4 for Synthesis Runs					
REACTION 11							
1730	77	gel	34.4	2140	950	53	SPh+Ne+(Fo?)+V
1731	73	gel	25.8	2140	950	53	Ne+SPh+V
1774	73	gel	30.5	2000	975	46	L+SPh+V+qNe+qSPh
1853	77	gel	35.4	2205	975	71	SPh+L+(Fo?)+V+qSPh

and have perfect basal cleavage. In oil-immersion mounts they are characterized by their platy six-sided habit, essentially parallel extinction, length-slow elongation, and low to moderate birefringence. Their refractive indices differ considerably, as indicated below, but more important at this point was the variation in grain size which they exhibited. Primary SPh from subsolidus runs was typically between 5 × 1 and 10 × 2 microns in size whereas in L-rich runs 1–2 micron platelets were typical of silica-rich liquid and 200 × 5 micron crystals in a very complex veined-structure were typical of less silica-rich liquids. Both were interpreted as having formed during the quench (see qSPh of Table 2). The finer products were associated with typical primary SPh. The coarser products were even more obvious because the typical cohesiveness of glass-rich pellets was often destroyed by the development of SPh and its subsequent hydration during the quench, leaving only a fragile relict, including a relict meniscus, which could easily be disaggregated by the touch of a needle point.

Crucial data for the upper stability of SPh are shown in Table 2 and, with other data, in Figure 1. Reaction 4 passes 818 ± 15°C at 250 bars, 864 ± 10°C at 500 bars to invariant point **H** at 874 ± 10°C and 530 ± 50 bars. A decrease in the amount of previously synthesized SPh by an order of magnitude in runs 1295, 2355, 1505, 2311, and 2350 was taken as evidence for its instability. Justifying this criteria was the lack of SPh synthesis from Fo+Ne+Ab+V beyond reaction 4 (run 2351). Run 2353 (see ?, Fig 1) is a contradiction that perhaps results because of synthesis during the quench or during run-up to *P* and *T* and metastable persistence (see Wones, 1967 for similar problems).

Invariant point **H** (Figs. 1 and 2) is a normal quaternary type IV of Schreinemakers (1915, p. 826). L is estimated to contain 1 wt percent H_2O (from Peters *et al*, 1966) and 67 ± 2 wt percent $NaAlSiO_4$, 32 ± 2 wt percent SiO_2 and 1 ± 0.5 wt percent Mg_2SiO_4 by its projection onto the anhydrous base. The vapor phase composition was not estimated. Chemographic relations of experimental data suggest some solid solution of albite in Ne (Fig. 2) but there was no evidence for any solid solution in Ab, Fo, or SPh. Reaction 5 was confirmed in the vicinity of **H** and may be considered to pass through 1058 ± 5°C at one bar (Schairer and Yoder, 1961, Fig. 35) as H_2O is added to the Mg_2SiO_4-$NaAlSiO_4$-SiO_2 system. Reaction 9 (Fig. 2) was determined to pass through 840 ± 10°C at 770 bars and 800 ± 10°C at 1150 bars using crystalline starting materials (Table 2). The nature and arrangement of reactions 7 and 8 (Fig. 2) is dictated by the composition of L which is positioned below the prolongation of the Ab+SPh+Fo plane and above the Ab+Ne+SPh plane. The position of reaction 7 was well documented (Table 2), but reaction 8 was not studied. Reaction 6 governs the upper stability of SPh above **H.** Critical runs 2281, 2279, 2408, 2141, and 2407 (Table 2) indicate that this reaction passes through 915 ± 10°C at 750 bars and 960 ± 15°C at 1100 bars (=**I**).

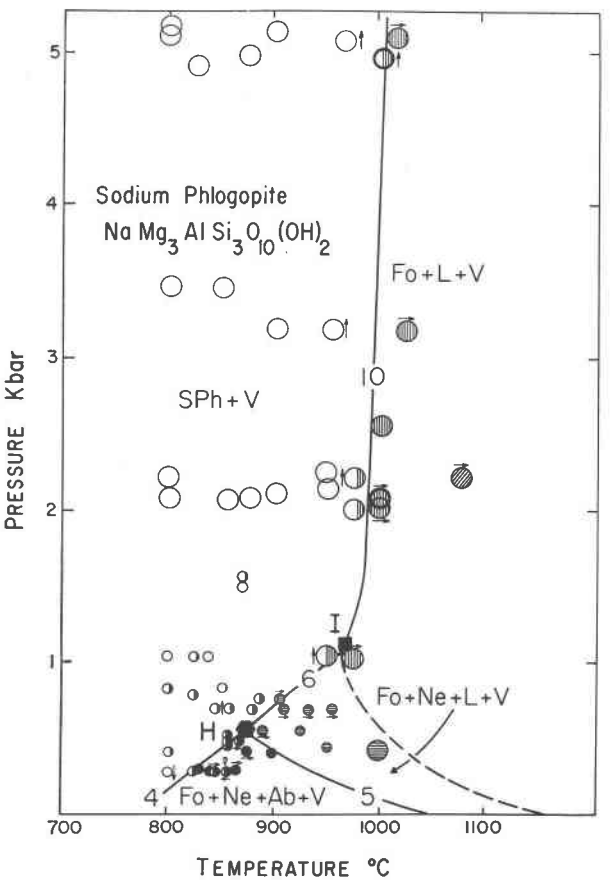

FIG. 1. Pressure-temperature projection of quench-run data showing invariant points (lettered), univariant reactions (solid lines, numbered), and divariant stability fields (symboled) pertaining to the upper stability of SPh for compositions along the SPh–H_2O join. A dashed line separates Ne+Fo+L+V from Fo+L+V for this join. Larger circular quench-run symbols for experiments in internally heated vessels, smaller for externally heated vessels. Left and upward pointing arrows by run symbols represent Fo+Ne+Ab+H_2O initially whereas right and downward pointing arrows represent SPh+H_2O initially. Other runs were gel+H_2O initially. Thickened symbols represent duplicate runs.

Invariant point **I** (Figs. 1 and 3) is of the variable singular type of Schreinemakers (1917, p. 999) where reaction 6 changes to reaction 10, which is ternary, and reaction 11, which is quaternary. It results as L of reaction 6 becomes more SiO_2-poor at the point when it coincides with the prolongation of the Fo+SPh+V plane (Fig. 3). Experimentally, Ne is present in the decomposition products below **I** but not above it. The invariant L at **I** is estimated to contain 82 ± 3 wt percent $NaAlSiO_4$, 16 ± 2 wt percent SiO_2 and 2 ± 1 wt percent Mg_2SiO_4. It probably contains less than 1 wt percent H_2O because of its *P-T* position relative to **H**, but this could not easily be determined because of quench problems. No significant deviations from presumed stoichiometry were evident for SPh, Ne, or Fo. The composition of V at **I** was not determined.

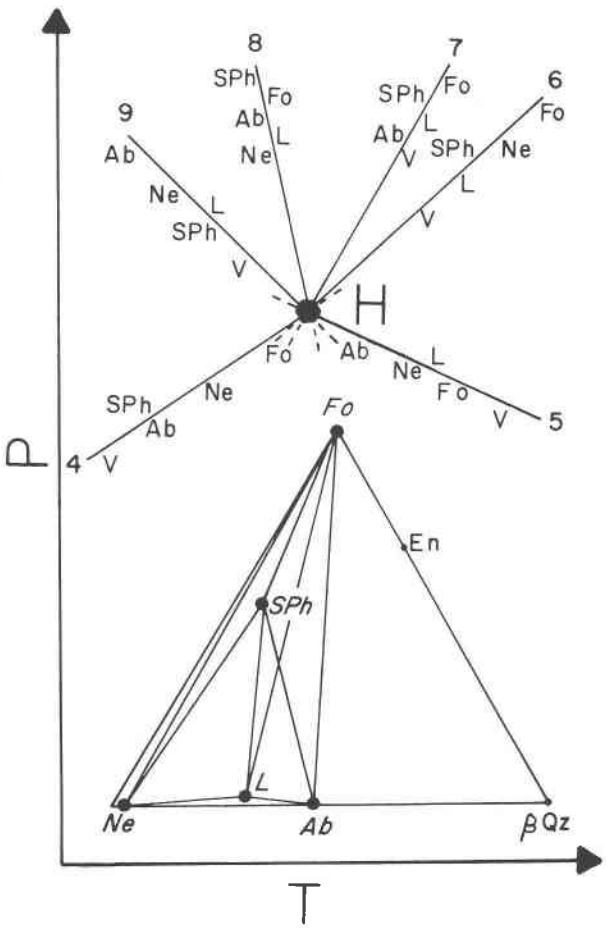

FIG. 2. Pressure-temperature projection of schematic array of univariant reactions about invariant point H. Chemographic relations of invariant phases; except vapor, shown in projection from the H_2O apex onto the $NaAlSiO_4$(Ne)–Mg_2SiO_4(Fo)–SiO_2(βQz) base.

Reaction 10 expresses the upper stability of SPh above **I**. Critical runs 1880, 1652, 1968, 1077, 1857, 1599, 1765, 1878, and 1653 (Table 2 and Fig. 1) indicate this reaction passes through 990 ± 10°C at 2000 bars and 1010 ± 10°C at 5000 bars. Because of abundant qSPh additional compositions were used to locate reaction 10. A broad primary field of SPh+L+V, at temperatures below reaction 10 (*e.g.*, runs 1866, 1867, and 1871), collapses to Fo+L+V, from both sides (richer and poorer in SiO_2), above it (*e.g.*, runs 1965, 1966, 1967, and 1969).

More details concerning these relations and other reactions of the $NaAlSiO_4$-Mg_2SiO_4-SiO_2-H_2O system are in preparation.

Pressure-DTA Data

Preliminary X-ray diffraction data at various temperatures indicated that the water-saturated upper stabilities of SPh HII and SPh HI and the lower stabilities of SPh and SPh HI could be determined using differential thermal analysis technique under controlled pressure. SPh HII (111.1 mg, run 2246 at 700 ± 6°C, 1000 bars for 62 hours using gel #80) plus 30 wt percent H_2O and quartz from Lake Toxaway (Keith and Tuttle, 1952) were used to determine reactions 1, 2, and 3 of Figure 4. As reasonable agreement with data of Yoder (1950) was attained for reaction 3, no corrections were applied to the raw data for reactions 1, 2, or 3. Equations for them may be written as $T = 5.4\ P + 82(\pm 2)$ for reaction 1 and $T = 17.4\ P + 328(\pm 2)$ for reaction 2 (where T is in °C and P is in kilobars). There is no evidence of curvature for these three reactions in the pressure range of 100 to 5000 bars.

Controlled Ignition Data

The measured masses of several samples (*ca* 50–300 mg) were allowed to equilibrate at atmospheric pressure and 6°C, 25°C (dry air), 80°C, and finally at 1000°C and then used to estimate the water contents of SPh, SPh HI, and SPh HII. The estimated H_2O content of SPh was 5.34 ± 1.0 wt percent, which is in reasonable agreement with 4.49 wt percent calculated for $NaMg_3AlSi_3O_{10}(OH)_2$. The experimental water contents for SPh HI and SPh HII were 13.1 ± 2.0 wt percent and 22.7 ± 1.0 wt percent, respectively. Using these water contents to infer integer nH_2O values for these hydrates, the following formulas and corresponding water contents are indicated: $NaMg_3AlSi_3O_{10}(OH)_2 \cdot 2\ H_2O$, 12.4 wt per-

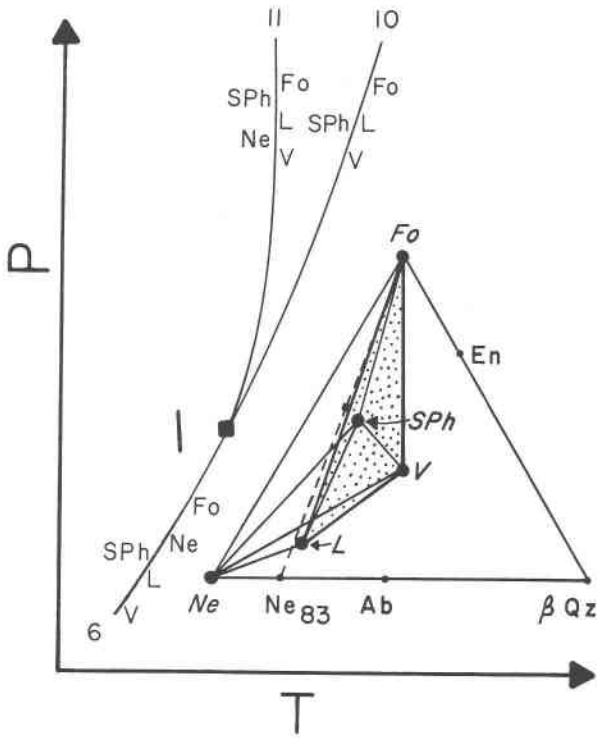

FIG. 3. Pressure-temperature projection of schematic array of univariant reactions about invariant point **I**. Chemographic relations of singular phases, SPh, Fo, L, and V shown as coplaner (dotted) within the $NaAlSiO_4$(Ne)–Mg_2SiO_4(Fo)—SiO_2(βQz)–H_2O(V) tetrahedron. Notice position of anhydrous SPh (square) on the Fo–Ne_{83} join for reference. The anhydrous composition of L lies essentially on this same join when projected from V.

cent H_2O for SPh HI, and $NaMg_3AlSi_3O_{10}(OH)_2 \cdot 5H_2O$, 22.0 wt percent H_2O for SPh HII.

Refractive Index Data

Refractive indices of SPh, SPh HI, and SPh HII were measured on material synthesized over a range of *P-T* conditions and run durations as well as by changes of *P-T* conditions on previously synthesized material (Table 3). Oils calibrated at 25°C using sodium light were used for these determinations in white light. Some unusual techniques were employed in the determinations for SPh and SPh HI. To attain SPh indices, SPh HII was heated to 80°C to dehydrate it to SPh and a small quantity (less than 1 wt percent re. oil) was introduced directly into oils of the desired range; cooling SPh to about room temperature yielded SPh HI for its determinations. There is no reason to suspect that the oils or SPh were adversely affected by mixing-in 80°C SPh. The temperature of the oil may increase by a degree, if that much, and X-ray diffractions of SPh in these oils reveal no structural complexing with them, nor is there any complexing of oils with SPh HI or with SPh HII. In fact these forms were also indifferent to the presence of ethylene glycol, a common complexing agent of sheet silicates.

Cell Parameter Data

Tables 4 and 5 give the X-ray powder diffraction data and cell parameters of SPh, SPh HI, and SPh HII at various temperatures. Pure spinel ($MgAl_2O_4$), supplied by G. V. Gibbs of Virginia Polytechnic Institute and State University, served as the internal standard for these data after correction for its thermal expansion using data of Rigby (in Clark, 1966, Table 6.1). The program of Evans, Appleman, and Handwerker (1963) was used for the structural refinement with the aid of unambiguously indexed spacings of a preliminary refinement. Only two of these indexed spacings—d_{060} for SPh HI and d_{011} for SPh—were rejected in the final refinement because of interference or error limits. Estimates of

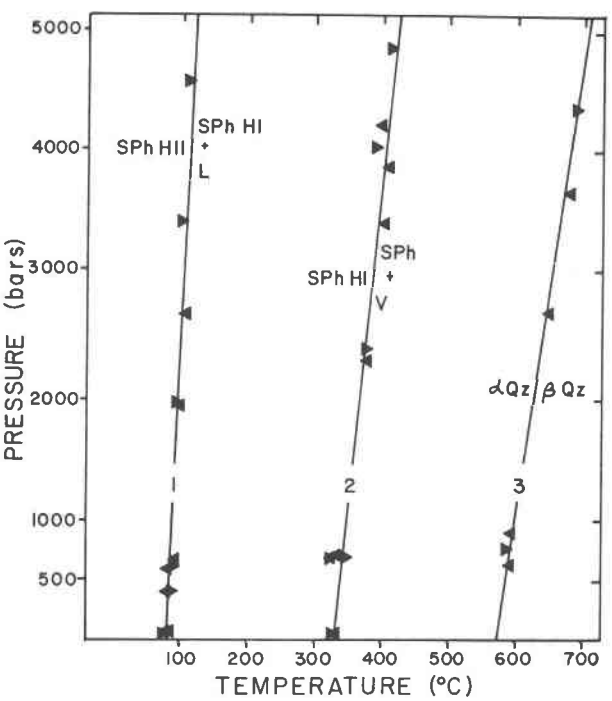

FIG. 4. Pressure-temperature projection of run data for reactions 1, 2, and 3 deduced by differential thermal analysis under pressure. Triangles point in direction of changing temperature for all three reactions. The slope and 1 bar intercept of reaction 3 are after Yoder (1950).

TABLE 3. Refractive Indices of SPh, SPh HI, and SPh HII from Quench Runs

Run No.	Comp No.	Start. Cond.*	P bars	Temp °C	Time Hr.	SPh γ = β	SPh α	SPh HI γ = β	SPh HI α	SPh HII γ = β	SPh HII α
1827	80	1634	828	874	59			1.546	1.537		
1453	80	gel	1030	800	24	1.572	1.542	1.550	1.540		
2310	81	gel	1030	800	106	1.569	1.548	1.546	1.537	1.521	1.505
1426	80	gel	1030	800	96			1.546	1.538		
1634	80	gel	1210	833	92	1.565	1.546	1.546	1.537	1.521	1.509
1734	80	1634	2140	950	53					1.521	1.506
1620	80	gel	4960	875	73					1.521	1.507
1765	80	gel	4960	1000	40					1.523	1.508
				AVERAGES		1.569	1.545	1.547	1.538	1.521	1.507
				RANGES		±.004	±.003	±.003	±.002	±.002	±.002

*Starting condition whether gel or previous run. Water added to all runs (5 to 35 wt.%).

space groups were made using Donnay and Nowacki (1954; Table 15) for indices assigned by the program of Evans *et al* (1963). These have not yet been checked using single crystals.

Discussion

Experimental Inferences

Experimental data presented indicate that SPh, SPh HI, and SPh HII are stable phases of the $NaAlSiO_4$-$MgSiO_2$-SiO_2-H_2O system whose oxide ratios are $Na_2O \cdot 6\,MgO \cdot Al_2O_3 \cdot 6\,SiO_2$ and which are related by binary reactions (1 and 2 of Figure 4) in the system $NaMg_3AlSi_3O_{10}(OH)_2$-H_2O. Using the data of Burnham, Holloway, and Davis (1969) the calculated increases in volume for their dehydrations are 5.47 Å^3/mole of SPh HII and 14.83 Å^3/mole of SPh HI at 2000 bars (96°C and 365°C, respectively) assuming no significant thermal expansion for SPh, SPh HI, and SPh HII relative to their molar volumes of Table 5. The calculated molar volumes of H_2O in SPh HII and SPh HI are 75.64 Å^3 or 15.13 Å^3/mole of H_2O and 28.91 Å^3 or 14.46 Å^3/mole of H_2O, respectively (Table 5). These values are significantly less than those for pure water at corresponding conditions.

The only inconsistency noted so far among these data concerns comparisons of calculated versus measured average refractive indices, using the relation of Gladstone and Dale (1864), specific refractive energies for oxides given in Larsen and Berman (1934, Table 2), calculated densities (Table 5), and the compositions deduced for SPh, SPh HI, and SPh HII. The differences between average refractive indices (calc *vs* meas) for SPh HII and SPh HI were 0.003 and 0.011, respectively. These are reasonable compared to differences calculated for talc, phlogopite, and alkali feldspars (0.005 to 0.010), but that for SPh (0.021) seems too high. This is, however, the minimum difference (in an absolute sense) when minor changes in water content, within the range of experimentally determined values, are considered.

In a similar study, Hazen and Wones (1972) suggested that $k(H_2O)$ in Larsen and Berman (1934) was too low. Perhaps a value for $k[(OH)_2]$ is needed.

Mineralogic Implications

Table 6 indicates minerals in which SPh HII, SPh HI, or SPh (all calculated as the anhydrous equivalent *SPh*) may be imagined as compositional end-members. The similarity in structures implied by this influence is more difficult to evaluate but qualitative similarities are good. For example, specimen B was shown to have variable hydration states whose basal spacings are 9.65 Å, 12.27 Å, and 14.92 Å. Its 15.49 wt percent total H_2O is probably representative of material with a 12.27 Å basal spacing. Similar data are not available for specimens C and D.

In a more general sense, the dehydration stages and corresponding H_2O losses for Mg-rich vermiculite determined by Walker (1951, 1957) are similar to those inferred for reactions 1 and 2 (Figure 4) and 4 (Figure 1): (1) −48 percent H_2O below 100°C (14.4 Å → 11.6 Å) *vs* −44 percent for reaction 1 (15 Å → 12 Å); (2) −25 percent H_2O between 250°C and 400°C (11.6 Å → 9.6 Å) *vs* −36 percent for reaction 2 (12 Å → 10 Å); and (3) −27 percent between 600°C and 850°C (9.6 Å → anhydrous phases) *vs* −20 percent for reaction 4 (10 Å → anhydrous phases). He attributed the first stage of dehydration [(1) above] to a loss of water "unbound" to interlayer Mg ions, the second [(2) above] to loss of water bound to Mg ions and the final dehydration [(3) above] to loss of (OH) ions from the octahedral layer of vermiculite. While Walker's structural interpretations seem reasonable for the general results of this study, the interpretation that stage 1 involves "unbound" water seems to be inconsistent with phase and structural considerations reported here.

The only minor conflict with the concept of SPh HII, SPh HI, and SPh as composition and structural end-members of vermiculite and its stages of hydration comes from Na-vermiculite formed using ion exchange by Barshad (1948). He found that it had only one interlayer of water and only one low temperature dehydration, but the relative humidity of

TABLE 4. Interplanar Spacings for SPh, SPh HI, SPh HII at 1 Atm and Various Temperatures†

SPh HII T = 25 ± 3°C				SPh HI T = 55 ± 5°C				SPh T = 130 ± 10°C			
hkl	*d* calc††	*d* obs†††	*I***	*hkl*	*d* calc††	*d* obs†††	*I***	*hkl*	*d* calc††	*d* obs†††	*I***
001*	*14.868*	14.841	VS	001*	*11.874*	12.006	S	001*	9.903	10.210	S
003	*4.956*	4.954	W	020*	*4.615*	4.614	M	020*	*4.601*	4.611	M
020*	*4.614*	4.629	M	004*	2.968	2.953	S	003*	*3.301*	*3.305*	SB
013	4.366	4.285	W	103	2.948			103	*2.634*	2.637	M
111	4.249			200	*2.599*	2.602	M	113	*2.532*	2.535	M
$\bar{1}12$	*4.116*	4.116	W	$\bar{1}24$	*2.367*	2.368	W	$\bar{1}23$	*2.499*	2.499	MB
022	*3.919*	3.929	WB	$\bar{2}03$	*2.334*	2.334	W	$\bar{2}12$	2.366		
$\bar{1}12$	3.720	3.718	W	$\bar{2}22$	*2.212*	2.209	W	104	2.363	2.341	M
$\bar{1}13$	3.573	3.553	VW	006	*1.979*	1.977	W	211	2.361		
120	3.475			$\bar{1}44$	1.769	1.769	W	040	2.301		
				106	1.766						
023	*3.376*	3.385	W					$\bar{2}23$	1.982		
$\bar{1}04$	3.245	3.213	W	$\bar{1}27$	*1.584*	1.585	W	005	1.981	1.980	W
113	3.191			225	1.544			$\bar{2}22$	1.977		
122	*3.050*	3.048	W	060	1.538	1.541	M	$\bar{1}42$	1.976		
005*	*2.974*	2.971	S	$\bar{1}54$	1.534			105	*1.774*	1.772	W
130	2.658	2.656	W	136	1.531	1.530	WB	144	1.562		
$\bar{1}24$	2.654			243	1.528			026	1.554	1.554	M
$\bar{2}02$	*2.599*	2.599	M	047	1.367			312	1.553		
$\bar{2}11$	2.558	2.561	M	064	1.366	1.365	M	060*	*1.534*	1.534	M
132	2.556			118	1.360			332	*1.402*	1.401	M
$\bar{1}33$	*2.409*	2.412	S								
$\bar{1}34$	2.232	2.233	VW								
214	2.321										
007	2.124	2.120	VW								
$\bar{2}05$	2.117										
$\bar{1}41$	2.108	2.107	VW								
126	2.104										
$\bar{1}35$	*2.049*	2.046	W								
$\bar{2}33$	1.925	1.926	VWB								
$\bar{2}25$	1.924										
037	1.748	1.748	VW								
127	1.747										
$\bar{1}52$	1.712	1.711	W								
241	1.709										
146	1.568										
055	1.568	1.568	W								
322	1.567										
$\bar{1}29$	*1.544*	1.545	W								
060*	1.537	1.536	W								

†*Cu radiation wavelength of 1.54178 used to calculate spacings greater than 2.885 Å, and 1.54050 used for lesser spacings.*

††d_{calc} *in angstroms for indexed monoclinic spacings. Italicized values were used to calculate cell parameters listed in Table 5.*

†††d_{obs} *in angstroms for measured spacings using spinel ($MgAl_2O_4$) as an internal standard.*

**Pre-indexed spacings for cell refinements.*

***Intensity of peaks : S = strong, M = medium, V = very, W = weak, and B = broad.*

his experimental conditions was not indicated. Possibly it was too low to stabilize a higher hydrate.

Further evaluation of this end-member concept with the behavior of vermiculite under hydrothermal conditions (Roy and Romo, 1957; Boettcher, 1966) is hampered by the fact that the stages of reversible hydration were not studied by them. However, both investigations encountered a quenchable 10 Å phase above 600°C. This phase could be structurally analogous to SPh if its water content were known.

The case for *SPh* as an end-member in montmorillonites (Table 6, analyses E and F) is less compelling because they have interlayer cation deficencies and, of the two sodium-rich analyses known, one is subaluminous (E) and the other is submagnesian (F). The fact that montmorillonites have interlayer cation deficiencies is not detrimental to this concept because Iiyama and Roy (1963b) refer to "ideal saponite" as $Na_{0.33}Mg_3Al_{0.33}Si_{3.67}O_{10}(OH)_2 \cdot nH_2O$ when it could be represented as 33 mole percent SPh and 67 mole percent talc, $Mg_3Si_4O_{10}(OH)_2$, if n were zero, or 33 mole percent SPh

TABLE 5. Cell Data for SPh, SPh HI, and SPh HII at 1 Atm and Various Temperatures*

	SPh T = 130±10°C	SPh HI T = 55±5°C	SPh HII T = 25±3°C
System	Monoclinic	Monoclinic	Monoclinic
Space Group	$P2_1/c$	$P2_1/m$	$P2_1/c$
a (Å)	5.265±.008	5.254±.007	5.330±.009
b (Å)	9.203±.006	9.229±.026	9.224±.006
c (Å)	9.994±.011	12.002±.011	14.996±.013
β angle	97° 45' ± 8'	98° 24' ± 11'	97° 28' ± 11'
Volume (Å^3)	479.8±0.8	575.8±1.9	730.0±1.5
Density**	2.777	2.522	2.232
Molar Vol.†	144.5	173.4	220.1

*Using observed data of Table 4 and refinement program of Evans et al. (1963).
**Density in grams /cm^3 assuming Z = 2 and that SPh = $NaMg_3AlSi_3O_{10}(OH)_2$, SPh HI = $NaMg_3AlSi_3O_{10}(OH)_2 \cdot 2H_2O$ and SPh HII = $NaMg_3AlSi_3O_{10}(OH) \cdot 5H_2O$.
†Molar volume = unit cell volume x Avogadio's number ÷ Z, assuming Z = 2.

HI if $n = 0.33 \times 2$ or 33 mole percent SPh HII if $n = 0.33 \times 5$. According to Ames and Sand (1959), Iiyama and Roy (1963a), Ernst (1961), and unpublished data of the author (Carman, 1969) water-expandable and ethylene glycol-expandable substances of such compositional representations do occur in the talc-SPh-H_2O plane. However, in light of this investigation, the higher levels of hydration mentioned by other investigators are probably attained during quenching by reactions like 1 and 2 (Figure 4) where talc-SPh HI and talc-SPh HII solid solution fields apparently exist. This would rationalize the similarities between the DTA patterns of synthetic montmorillonites of alleged high thermal stability (Iiyama and Roy, 1963a, Fig. 7) with those of natural montmorillonites (see Deer, Howie, and Zussman, 1962, Fig. 51; Grim, 1968, Fig. 9-9).

Two studies on the dehydration of montmorillonite under pressure are known. Ca-rich montmorillonite, studied by Stone and Rowland (1955), using DTA at pressures between one and 6 bars, had an initial dehydration of 150°C with a positive slope of 15°C/bar and a second dehydration at 200°C with a positive slope of 13°C/bar. These one bar intercepts and slopes are in general agreement with this study but differ in detail with it and with the study by Khitarov and Pugin (1966) on montmorillonite. Their experiments between 1.25 and 15 kbar revealed an intercept of 130°C at one bar and a positive slope of 9.3°C/kbar, for material of 15.8 Å basal spacing (20.04 wt percent H_2O) transforming to either material of 13.5 Å basal spacing (11.27 wt percent H_2O) or material of 9.6 Å basal spacing (5.29 wt percent H_2O). Except for the fact that these dehydrated phases were quenchable and the fact that only one (or two very close) dehydration reaction was inferred, these data are in good agreement with this investigation and support the suggested end-member relation of SPh HII, SPh HI, and SPh in montmorillonites of similar hydration.

Analysis G of Table 6 and structural comparisons of SPh with synthetic phlogopites (Table 7) suggest SPh could be an important end-member in phlogopites and biotites. Aside from differences in space group, phlogopites of Table 7 are 1*M* or 3*T*, cell parameters of SPh differ from phlogopite in a reasonable manner (see Hazen and Wones, 1972, Figs. 2, 4 and 5). However, typical phlogopites and biotites (Fig. 5) contain much less sodium than analysis G, Table 6.

Several reasons for this low amount of sodium in phlogopites and biotites and for the absence of sodium-rich phlogopites may be offered. First, it seems that sodium is fractionated toward other sodium-bearing minerals more strongly than toward phlogopite and biotite. This was noted by Goldschmidt (1916) in his study of trondjemites, confirmed by Nockolds (1947) in a more general study, and extensively documented for rocks of the Sierra Nevada batholith by Dodge *et al* (1968, 1969). Experimental evidence of this fractionation comes from Rutherford (1969, Figs. 6, 7) in his study of iron biotite-alkali feldspar equilibria. His data indicate that albite-rich feldspar coexists with annite ($KFe_3AlSi_3O_{10}(OH)_2$) with only 20 mole percent sodium annite ($NaFe_3AlSi_3O_{10}(OH)_2$) (see Weidner and Carman, 1968) at 2,000 bars, low f_{O_2}, and temperatures of 500 to 660°C.

Secondly, according to the results of this investigation, if sodium-rich phlogopites and biotites formed naturally they would tend to hydrate at lower temperatures in contact with water-rich fluids. Furthermore, since natural analogs of SPh HII and SPh HI are unknown and minerals enriched in either of these end-members are rare, it seems that an unusual natural environment may be required for them. For example, Weaver (1958) found that detrital montmorillonites and vermiculites were converted to potash-rich clays in sea water in spite of its sodium-rich composition.

TABLE 6. Potential *SPh* in Natural Minerals

Oxides	SPh	Natural Minerals (wt.%) B	C	D	E	F	G
SiO_2	47.03	43.80	29.96	30.51	63.65	64.47	37.32
TiO_2		1.09				.12	2.96
Al_2O_3	13.31	15.76	38.78	38.84	.71*	23.42	15.84
Fe_2O_3		10.15	1.30	1.45		4.27	2.78
FeO		.28	2.52	2.46		.35	1.62
MnO		.13					
MgO	31.57	22.95	17.94*	17.79*	30.05	2.90*	28.93
CaO		.33			.62	.58	
Na_2O	8.09	4.80*	6.96	6.45	3.56	3.20	3.75*
K_2O		.52	2.54	2.50	.08	.70	6.80
Li_2O			Tr	Tr	1.33		
P_2O_5		.19					
Total	100.00	100.00	100.00	100.00	100.00	100.01	100.00
H_2O Total†	(Below)	15.49	4.00	3.32	15.52	14.70	5.04
Potential SPh*		59%	57%	57%	5%	9%	46%

SPh Anhydrous SPh of this study, $Na\ Mg_3\ Al\ Si_3\ O_{11}$. The total H_2O is 4.49 for SPh, 12.4 for SPh HI or 22.0 for SPh HII.

B) Sodium Vermiculite, Unst, Shetland of Curtis, Brown and Somogyi, 1969, Table 3, specimen U8.

C) Vermiculite, Shooting Creek, Clay County, N. Carolina of Pratt and Lewis; 1905 p. 322 (Anal. Keonig, 1873).

D) Vermiculite, Buck Creek, Clay County, N. Carolina of Pratt and Lewis, 1905 p. 322 (Anal. Koenig, 1873).

E) Hectorite, Hector, California of Foshag and Woodford, 1936 (Anal. Foshag, excluding 0.31 Cl).

F) Montmorillonite, Upton Wyoming of Ross and Hendricks (1945).

G) Phlogopite, violet-brown plates in limestone, Monte Braccia, Val Malenco, Italy from Pagliani, 1940. (As recorded in Deer, Howie, and Zussman, 1962, Table 10).

†H_2O Total is sum of H_2O^- and H_2O^+ from analyses.

*Potential SPh for analyses B through G, limiting oxides indicated by *, eg. for anl. B, wt.% potential SPh = 4.80/8.09 x 100.

Conclusion

Previous studies in this system which indicate montmorillonites of unusually high thermal stabilty must be reinterpreted because the hydration states of at least some of these run products are probably attained during quenching.

In spite of the fact that sodium phlogopite and its hydrates do not naturally occur in pure form, there is enough chemical evidence and structural similarities between them and phlogopites, biotites, vermiculites, and montmorillonites to suggest that they may serve as useful end-members in the interpreta-

TABLE 7. Comparison of SPh with Synthetic Phlogopites

	a(Å)	b(Å)	c(Å)	Beta Angle	Volume (Å^3)
Ph†	5.31	9.20	10.31	99° 54'	497.0
Ph††	5.33	9.21	10.31	100° 10'	497.8
Ph†††	5.31	9.21	10.31	99° 53'	497.3
Ph*	5.32	9.21	10.31	99° 64'	497.3
SPh**	5.26	9.20	9.99	97° 45'	479.8
%Diff.***	-1.1%	-0.1%	-3.1%	-2.3%	-3.5%

† Phlogopite cell parameters after Yoder & Eugster (1954).
†† Phlogopite cell parameters after Wones (1963).
††† Phlogopite cell parameters after Luth (1967).
* Average for Phlogopite from the three determinitions above it.
** SPh of this investigation, Table 5.
*** % Difference=SPh-Av Ph/Av Ph x 100.

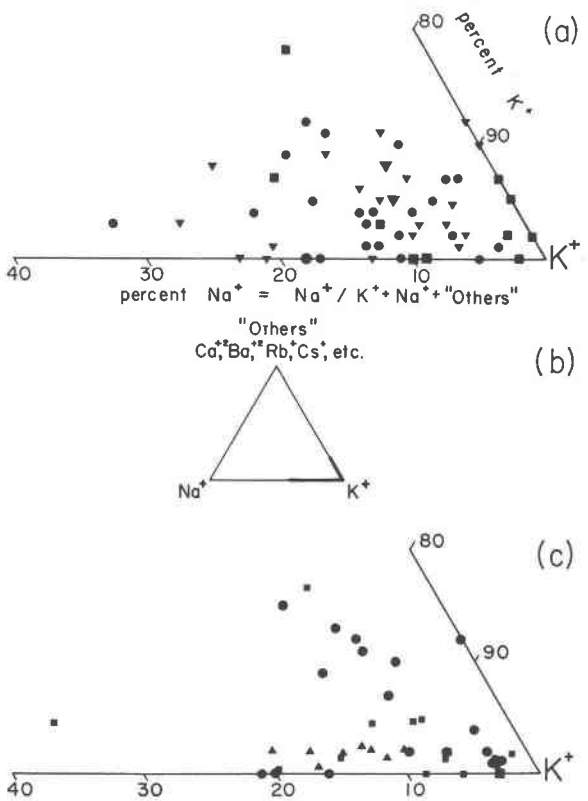

FIG. 5. Atom percent occupancy of interlayer positions of phlogopites and biotites based on structural formulas of analyzed specimens.

a) Phlogopites from Deer, Howie, and Zussman (1962, Table 10) represented as squares. From Foster (1964, Table 4) phlogopites and magnesium biotites represented as circles and ferrous biotites, siderophyllites, and lepidomelanes represented as inverted triangles.

b) Three end-members for interlayer occupancies shown in (a) and (c). Heavy weight lines in K^+ corner represents portions represented in (a) and (c).

c) Biotites from igneous rocks represented as circles (Deer *et al,* 1962, Table 12), biotites from metamorphic rocks represented as squares (Deer *et al,* 1962, Table 13), and biotites from salic volcanic rocks represented as triangles (Carmichael, 1967, Table 6). Notice that in both (a) and (c) coincident analyses represented by larger symbols.

tion of the physical, chemical, and genetic aspects of these natural sheet silicates. Hazen and Wones (1972) have recently used the data of this study toward these objectives in their investigation of substitution in synthetic trioctahedral micas, revising the earlier considerations of Radoslovich (1963).

Acknowledgments

In particular, I thank O. F. Tuttle, who suggested the $NaAlSiO_4$-Mg_2SiO_4-SiO_2-H_2O system for study. He provided inspiration, intriguing suggestions, thoughtful discussion, and crucial encouragement, and his grants through the National Science Foundation provided financial support for this study.

J. R. Weidner is acknowledged for hours of assistance during crucial experiments herein and for his valued discussions, as are W. C. Luth, A. L. Boettcher, R. H. Jahns, M. L. Keith, and D. M. Roy.

Special thanks are offered to A. E. Beswick, A. L. Boettcher, G. R. McCormick, R. H. Hoppin, and D. R. Wones who materially improved the present manuscript.

References

AMES, L. L., AND L. B. SAND (1958) Factors affecting maximum hydrothermal stability in montmorillonites. *Am. Mineral.* **43,** 641–648.

BARSHAD, I. (1948) Vermiculite and its relation to biotite as revealed by base exchange reactions, X-ray analysis, differential thermal curves, and water content. *Am. Mineral.* **33,** 655–678.

BOETTCHER, A. L. (1966) Vermiculite, hydrobiotite, and biotite in the Rainy Creek igneous complex near Libby, Montana. *Clay Minerals,* **6,** 282–296.

BURNHAM, C. W., J. R. HOLLAWAY, AND N. F. DAVIS (1969) The specific volume of water in the range 1000–8900 bars, 20° to 900° C. *Am. J. Sci.* **267-A,** 70–95.

CARMAN, J. H. (1969) *The Study of the System $NaAlSiO_4$-Mg_2SiO_4-SiO_2-H_2O from 200 to 5,000 Bars and 800°C to 1,100°C and Its Petrologic Applications.* Ph.D. Thesis, The Pennsylvania State University.

CARMICHAEL, IAN S. E. (1967) The iron-titanium oxides of salic volcanic rocks and their associated ferromagnesian silicates. *Contrib. Mineral. Petrol.* **14,** 36–64.

CLARK, S. P., JR. (1959) Effect of pressure on the melting points of eight alkali halides. *Chem. Phys.* **31,** 1526–1531.

——— (1966) *Handbook of Physical Constants. Geol. Soc. Am. Mem.* **97.**

CURTIS, C. D., P. E. BROWN, AND V. A. SOMOGYI (1969) A naturally occurring sodium vermiculite from Unst, Shetland. *Clay Minerals,* **8,** 15–19.

DEER, W. A., R. A. HOWIE, AND J. ZUSSMAN (1962) *Rock Forming Minerals.* Vol. 3. *Sheet Silicates.* John Wiley and Sons, New York.

DODGE, F. C. W., J. J. PAPIKE, AND R. E. MAYS (1968) Hornblendes from granitic rocks of the central Sierra Nevada batholith, California. *J. Petrol.* **9,** 378–410.

———, V. C. SMITH, AND R. E. MAYS (1969) Biotites from granitic rocks of the central Sierra Nevada batholith, California. *J. Petrol.* **10,** 250–271.

DONNAY, J. D. H., AND W. NOWACKI (1954) *Crystal Data. Geol. Soc. Am. Mem.* **60.**

ERNST, W. G. (1960) The stability relations of magnesioriebeckite. *Geochim. Cosmochim. Acta,* **19,** 10–40.

——— (1961) Stability relations of glaucophane. *Am. J. Sci.* **259,** 735–765.

EUGSTER, H. P., AND D. R. WONES (1962) Stability relations of the ferruginous biotite, annite. *J. Petrol.* **3,** 82–125.

EVANS, H. T., JR., D. E. APPLEMAN, AND D. S. HANDWERKER (1963) The least squares refinement of crystal unit cells with powder diffraction data by an automatic computer indexing method (abstr.). *Progr. Annu. Meet. Crystallogr. Assoc.* 42–43.

FOSHAG, W. F., AND A. O. WOODFORD (1936) Bentonitic magnesian clay-mineral from California. *Am. Mineral.* **21,** 238–244.

FOSTER, M. D. (1964) Water content of micas and chlorites, *U.S. Geol. Surv. Prof. Pap.* **474-F.**

GILLERY, F. H. (1959) Adsorption-desorption characteristics of synthetic montmorillonoids in humid atmospheres. *Am. Mineral.* **44,** 806–818.

GLADSTONE, J. H., AND T. P. DALE (1863) Researches on the refraction, dispersion, and sensitiveness of liquids. *Roy. Soc. London Philos. Trans.* **153,** 317–343.

GOLDSCHMIDT, V. M. (1916) Geologisch-petrographische studien im hochgebirge des sudlichen Norwegens, IV, Uberschicht der eruptivgesteine im kaledonischen gebirge zwischen Stavanger und Trondhjem. *Vidensk, selsk, Cristiania. Skrifer* I. *Mat.-Naturvidensk Kl.* **2,** 1–140.

GRIM, R. E. (1968) *Clay Mineralogy*. Second ed. McGraw-Hill Book Co., New York.

HAZEN, R. M., AND D. R. WONES (1972) The effect of cation substitutions on the physical properties of trioctahedral micas. *Am. Mineral.* **57,** 103–129.

IIYAMA, J. T., AND R. ROY (1963a) Controlled synthesis of heteropolytypic (mixed-layer) clay minerals. *Clays Clay Minerals,* Pergamon Press, New York, 4–22.

———, AND ——— (1963b) Unusually stable saponite in the system Na_2O-MgO-Al_2O_3-SiO_2. *Clay Minerals Bull.* **5,** 161–171.

KEITH, M. L. AND O. F. TUTTLE (1952) Significance of variation in the high-low inversion of quartz. *Am. J. Sci.* **250-A,** 203–280.

KHITAROV, N. L., AND V. A. PUGIN (1966) Behavior of montmorillonite under elevated temperatures and pressures. *Geokhimiya,* **7,** 790–795. [transl. *Geochem. Int.* **3,** 621–626 (1966)].

KOIZUMI, M., AND R. ROY (1959) Synthetic montmorillonoids with variable exchange capacity. *Am. Mineral.* **44,** 788–805.

KUSHIRO, I. (1972) Effect of water on the composition of magmas formed at high pressure. *J. Petrol.* **13,** 311–334.

LARSEN, E. S., AND H. BERMAN (1934) The microscopic determination of the nonopaque minerals. Second Ed. *Geol. Surv. Bull.* **848,** 265 pp.

LUTH, W. C. (1967) Studies in the system $KAlSiO_4$-Mg_2SiO_4-SiO_2-H_2O: I. Inferred phase relations and petrologic applications. *J. Petrol.* **8,** 372–416.

———, AND C. O. INGAMELLS (1965) Gel preparation of starting materials for hydrothermal investigation. *Am. Mineral.* **56,** 255–258.

NOCKOLDS, S. R. (1947) The relation between chemical composition and paragenesis in the biotite micas of igneous rocks. *Am. J. Sci.* **245,** 401–420.

PAGLIANI, G. (1940) Flogopite e titanolivina di Monte Braccio (Val Malenco). *Atti. Soc. Ital. Sci. Nat. Mus. Civ. Milano,* **79,** 20–22.

PETERS, T. J., W. C. LUTH, AND O. F. TUTTLE (1966) The melting of analcite solid solutions in the system $NaAlSiO_4$-$NaAlSi_3O_8$-H_2O. *Am. Mineral.* **51,** 736–753.

PRATT, J. H., AND J. V. LEWIS (1905) Corundum and the peridotites of western North Carolina. *North Carolina Geol. Surv.* **1,** 464 pp.

RADOSLOVICH, E. W. (1963) The cell dimensions and symmetry of layer lattice silicates: V. Composition limits. *Am. Mineral.* **48,** 348–367.

ROSS, C. S., AND S. B. HENDRICKS (1945) Minerals of the montmorillonite group. *U.S. Geol. Surv. Prof. Pap.* **205 B,** 79 pp.

ROY, R. (1956) Aids in hydrothermal experimentation: II. Methods of making mixture of both "dry" and "wet" phase-equilibrium studies. *J. Am. Ceram. Soc.* **39,** 145–146.

———, AND L. A. ROMO (1957) Weathering studies 1. New data on vermiculite. *J. Geol.* **65,** 605–610.

RUTHERFORD, M. J. (1969) An experimental determination of iron biotite-alkali feldspar equilibra. *J. Petrol.* **10,** 381–408.

SCHAIRER, J. F., AND H. S. YODER, JR. (1961) Crystallization in the system nepheline-forsterite-silica at 1 atmosphere pressure. *Carnegie Inst. Washington Year Book,* **60,** 141–144.

SCHREINEMAKERS, F. A. H. (1915–1925) In-, mono-, and divariant equilibria. *Koninkl. Akad. Van Welenschappen Te Amsterdam Proc.,* English ed., v. **18–28,** Ed. 18–28. Reprinted 1965, The Pennsylvania State University, University Park, Pa., 322 pp.

STONE, R. L., AND R. A. ROWLAND (1955) DTA of kaolinite and montmorillonite under water vapor pressures up to six atmospheres. *Clays Clay Minerals, 3rd Nat. Conf., NAS-NRC,* **395,** 103–116.

TUTTLE, O. F. (1949) Two pressure vessels for silicate-water studies. *Geol. Soc. Am. Bull.* **60,** 1727–1729.

WALKER, G. F. (1951) Vermiculite and some related mixed-layer minerals. *X-ray Identification and Structures of Clay Minerals,* chapter VII, pp. 199–223, *Mineral. Soc. G. B. Monogr.*

——— (1957) The vermiculite minerals. In, *The Differential Thermal Investigation of Clays,* chapter VII, pp. 191–206, Mineralogical Soc., London.

WEAVER, C. E. (1958) The effects and geologic significance of potassium "fixation" by expandable clay minerals derived from muscovite, biotite, chlorite, and volcanic materials. *Am. Mineral.* **43,** 839–861.

WEIDNER, J. R., AND J. H. CARMAN (1968) Synthesis and stability of sodium annite, $NaFe_3AlSi_3O_{10}(OH)_2$ (abstr.). *Annu. Meet. Geol. Soc. Am. Program,* p. 315.

WINCHELL, A. N., AND H. WINCHELL (1964) *The Microscopic Characters of Artificial Inorganic Solid Substances: Optical Properties of Artificial Minerals.* 3rd ed., Academic Press, New York.

WONES, D. R. (1963) Physical properties of synthetic biotites on the join phlogopite-annite. *Am. Mineral.* **48,** 1300–1321.

——— (1967) A low pressure investigation of the stability of phlogopite. *Geochim. Cosmochim. Acta,* **31,** 2248–2253.

YODER, H. S., JR. (1950) High-low quartz inversion up to 10,000 bars. *Am. Geophys. Union Trans.* **31,** 827–835.

———, AND H. P. EUGSTER (1954) Phlogopite synthesis and stability range. *Geochim. Cosmochim. Acta,* **6,** 157–185.

Manuscript received, June 25, 1973; accepted for publication, October 26, 1973.